Microelectronics Reliability 124 (2021) 114290

Contents lists available at ScienceDirect

Microelectronics Reliability

journal homepage: www.elsevier.com/locate/microrel

Thickness and metallization layer effect on interfacial and vertical cracking of sintered silver layer: A numerical investigation

Fei Qin [a,b], Shuai Zhao [a], Lingyun Liu [a], Yanwei Dai [a,b,*], Tong An [a,b], Pei Chen [a,b], Yanpeng Gong [a,b]

[a] Institute of Electronics Packaging Technology and Reliability, Faculty of Materials and Manufacturing, Beijing University of Technology, Beijing 100124, China
[b] Beijing Key Laboratory of Advanced Manufacturing Technology, Beijing University of Technology, Beijing 100124, China

ARTICLE INFO

Keywords:
Cracking
Sintered silver
Energy release rate
Metallization layer
Porosity effect

ABSTRACT

Cracking of sintered silver layer always leads to the reliability issues in power devices. In this paper, the cracking behaviors of sintered silver layer have been investigated through numerical analysis with fracture based method. Energy release rate of various interfacial cracks and vertical cracks in sintered silver are computed. It is found that the energy release rate of interfacial crack and vertical crack are significantly influenced by their thickness. The thinner of the sintered silver layer, the higher of the energy release rate it will meet. For interfacial crack, the adding of the metallization layer does not improve the energy release rate significantly. For vertical crack, two conditions are considered, i.e., vertical crack emanating from the chip sider or emanating from the copper baseplate side, and it is found that the energy release rate is strongly dependent on its location and the existence of metallization layer. The increase of the thickness of Ni layer enables to lower down the entire level of energy release rate for vertical crack. Otherwise, the energy release rate of vertical crack near the edge region of the sintered silver layer is much higher than other locations. It implies that the cracking risk is higher for thinner sintered silver layer around the edge region which should be avoided. It is also found that the porosity effect on interface cracking and vertical cracking of sintered silver is also important.

1. Introduction

Sintered silver is very promising to be adopted as the die attach material for high temperature aimed power electronics of next generation in recent years [1–4]. Similar to study of the cracking of the traditional solder joint [5,6], cracking of sintered silver is also one of the main focus because of the reliability issue for the electronic devices, which has recently drawn great attentions [7–11]. Different cracking morphologies have been found for sintered silver layer in different experimental and numerical works [7–11], however, for the most of the cases, it is hard to give a reasonable explanations on them as most of the investigations differ from each other to some extent.

Herboth et al. [7] made an experimental investigation and found the cracking starts from the die corner, then the crack grows through the interlayer of sintered silver after 1250 thermal cycles. Different from Herboth et al. [7], Kraft et al. [8] performed an active thermal test which shows that the crack in the sintered silver grows vertically, and some cracks even grow down forward to the copper substrate layer. Another important information that we can obtain form Kraft et al. [8] is that effect of metallization is also important on the cracking of sintered silver layer. To further reveal the morphology of the crack initiation in sintered silver considering creep effect, Tan et al. [9] performed a 3D x-ray visualization observation and the creep crack is dominated along the interface region of the sintered silver layer. A more recent observation of cracking of sintered silver is presented by Agyakwa and coworkers [12], complicated crack network morphology of sintered silver layer is clearly shown in their study.

Regardless of active thermal test or passive thermal test of sintered silver, it should be related with thermal fatigue or thermal mechanical fatigue in essence. Noting this point, Tan et al. [13], Shioda et al. [14], Kimura et al. [15], and Osaki et al. [16] have studied the fatigue crack propagation of sintered silver where classic fatigue theories have been brought in such as concepts of inelastic strain energy density and cyclic *J*-integral [14]. Rather than studies on fatigue for sintered silver, the

* Corresponding author at: Institute of Electronics Packaging Technology and Reliability, Faculty of Materials and Manufacturing, Beijing University of Technology, Beijing 100124, China.
E-mail address: ywdai@bjut.edu.cn (Y. Dai).

https://doi.org/10.1016/j.microrel.2021.114290
Received 10 April 2021; Received in revised form 10 July 2021; Accepted 18 July 2021
Available online 3 August 2021

fracture behaviors of sintered silver have also drawn the attentions. Wang et al. [17] performed a fracture test through compact tension cracked sintered silver specimen. Chen and coworkers [18,19] investigated the macro and micro fracture toughness of sintered silver as well as the effect of different metallization layers. Recently, the influences of crack on the equivalent thermal conductivity were reported by our group [20]. One of the greatest challenge to analysis the cracking behavior of sintered silver is that the mechanical behaviors of sintered silver is significantly dependent on its porosity [21,22]. Some experimental results have verified this point, e.g. Wereszczak et al. [23] presented that Young's modulus and Poisson's ratio is a function of porosity. Those factors will surely affect the stress intensity and failure modes of sintered silver [24,25].

Although some efforts have been made to investigate the cracking problem of sintered silver, some important topics are still not touched in depth. Some confusions always exist, e.g., does the cracking should be influenced by its thickness and to what extent? Vertical cracking and interfacial delamination which would be more dangerous? Are there some guidelines can be provided to reduce the cracking risk of sintered silver by structure design or by adding different metallization layer? In this paper, those confusions will be answered from a perspective of fracture mechanics.

Toward this end, the organizations of this paper are arranged as the following. The problem to be investigated will be stated in Section 2. The interfacial cracking and vertical cracking behaviors and the detail comparisons are studied in Section 3 and Section 4, respectively. The discussions will be given in Section 5, and the concluding remarks will be drawn in the last Section.

2. Problem statement, methodology and numerical procedures

2.1. Model description and materials property

In general, a typical “sandwich” liked SiC chip/sintered silver layer/copper baseplate structure is presented as shown in Fig. 1. For most of the conditions, the back of the SiC chip is sputtered with metallization layer such as nickel (Ni) layer, silver (Ag) layer and so on. To enhance the adhesive forces, the top of the copper (Cu) baseplate is also metallized with gold (Au) layer and Ni layer.

The geometry parameters such as interfacial crack length, vertical crack length, sintered silver thickness, width of the chip length, metallization layer thickness on the backside of SiC chip and metallization layer thickness on the topside of copper baseplate for the structures shown in Fig. 1 are denoted as a_1, a_2, h_3, w, t_1 and t_2, respectively. During the calculations, a simplified geometry model is shown where it comes from the real size of a SiC power module in a commercial new energy electric vehicle. The width and thickness of the SiC chip are kept as 2.3 mm and 0.18 mm, respectively. The width and thickness of the Cu substrate is 9.05 mm and 0.7 mm, respectively. The width of sintered silver layer is same as that of SiC chip. The thickness of sintered silver layer and metallization layer varies accordingly.

Considering the cracking behavior of the sintered silver presented in different experiments, four different kinds of crack locations are adopted to perform the simulation. First kind, the crack is assumed to appear on the interface of SiC chip and sintered silver layer. The crack bonding between copper baseplate and sintered silver layer is assumed to be the second kind. The third kind of crack is assumed to lay vertically in sintered silver layer and emanating from the SiC side. The fourth kind of crack is assumed to distribute vertically in sintered silver layer and emanating from the copper baseplate. Those four kinds of crack types are the mainly possible crack types appearing in sintered silver layer. The finite element model is based on those defined four kinds of crack locations. The material properties are summarized in Table 1 where the material properties are collected from the published references listed in Table 1.

Noted that Young's modulus and Poisson's ratio are dependent on porosity based on the solutions given by Wereszczak et al. [23], e.g. Young's modulus is 72 GPa with porosity of 3–4% and Young's modulus is 58 GPa at porosity 7%. If the porosity increases to 19%, the Young's modulus is 40 GPa. For the influence of porosity on Poisson's ratio, a fitting formula has been given by Wereszczak et al. [23], some of which have been listed in Table 2. There are also other data about the porosity effect on the Young's modulus and Poisson's ratio in which can be found in the review article recently presented by Chen and Kim [21].

Table 1
Material properties adopted in the simulations.

Material	Young's modulus (MPa)	Poisson's ratio	CTE (ppm/°C)	References
Sintered silver	12,900	0.1	19.2	[26]
SiC	430,000	0.17	4.1	[27]
Cu	99,800	0.34	16.5	[27]
Ag film	76,800	0.37	18.9	[28,29]
Ni film	200,000	0.31	13.4	[26]
Au film	82,900	0.42	14.3	[28,29]

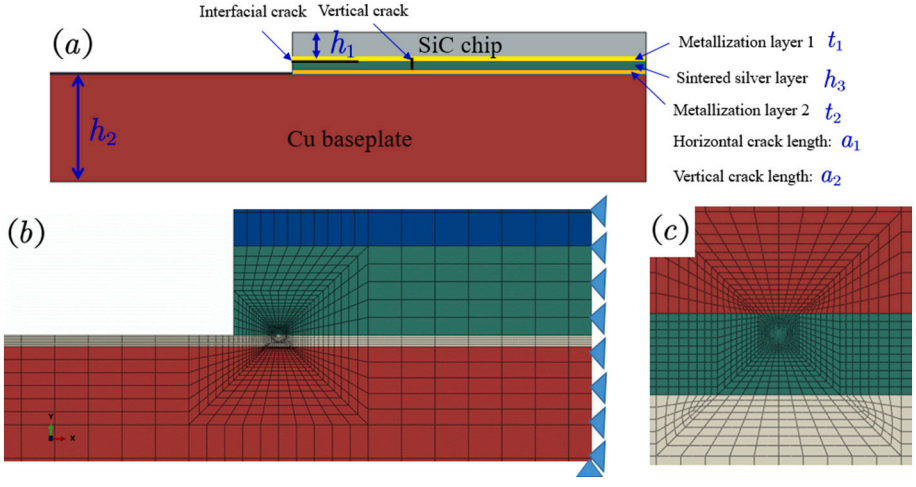

Fig. 1. Geometry model and finite element meshes for SiC/sintered silver/copper baseplate structures: (a) geometry model, (b) entire FE mesh and (c) crack tip mesh.

Table 2
Young's modulus and Poisson's ratio under different porosities [23].

Porosity	Young's modulus (MPa)	Poisson's ratio
3–4%	72,000	0.37
19%	40,000	0.28
38%	14,000	0.20

2.2. Methodology and numerical procedures

To characterize the interface crack of two bonding materials, the two Dundurs parameters α and β are defined as following:

$$\alpha = \frac{\widehat{E}_1 - \widehat{E}_2}{\widehat{E}_1 + \widehat{E}_2} \tag{1}$$

$$\beta = \frac{\mu_1(\xi_2 - 1) - \mu_2(\xi_1 - 1)}{\mu_1(\xi_2 + 1) + \mu_2(\xi_1 + 1)} \tag{2}$$

where $\widehat{E}_1$ and $\widehat{E}_2$ are the equivalent elastic modulus, and they satisfy $\widehat{E}_i = E_i/(1-\nu_i^2)$ and $\xi_i = 3 - 4\nu_i$ for plane strain condition. There will be $\widehat{E}_i = E_i$ under plane stress condition. Herein, E_i and ν_i are Young's modulus and Poisson's ratio for i-th material, respectively. The subscripts 1 and 2 represent the two bonding materials.

For interface crack, the oscillatory singularity index is defined as below:

$$\varepsilon = \frac{1}{2\pi} ln\left(\frac{1-\beta}{1+\beta}\right) \tag{3}$$

With the defined oscillatory singularity index, the energy release rate, G, of an interface crack along the bonding materials is defined as.

$$G = \frac{1}{2}\left(\frac{1}{\widehat{E}_1} + \frac{1}{\widehat{E}_2}\right)\frac{|K|^2}{cosh^2(\pi\varepsilon)} \tag{4}$$

in which

$$|K|^2 = K_{\mathrm{I}}^2 + K_{\mathrm{II}}^2 \tag{5}$$

And, the following relation is given.

$$cosh^2(\pi\varepsilon) = \frac{1}{1-\beta^2} \tag{6}$$

The mode mixity or phase angle ψ is defined as following:

$$\psi = tan^{-1}\left(\frac{K_{\mathrm{II}}}{K_{\mathrm{I}}}\right) \tag{7}$$

where K_{I} and K_{II} are the stress intensity factors of mode I and mode II, respectively.

To simulate the cracking of the sintered silver under thermal loading, the energy release rate of various kinds of cracking types will be analyzed. The applied temperature loading varies between 25 °C and 250 °C and the stress free reference temperature is set as 25 °C.

To obtain the energy release rate of the interface crack under various conditions, the interaction integral method implemented in commercial software ABAQUS is adopted. The energy release rate of the interface crack tip field can be obtained directly through extraction. A more detail method to simulate the crack tip can be found in our previous investigation [30]. The typical FE mesh of a crack front is given in Fig. 1(c). The solution extracted from integral of contour is a robust method which can maintain a fine accuracy.

3. Results

3.1. Interfacial cracking of sintered Ag/SiC interface

Herein, the first cracking condition is considered. The crack is assumed to be along the interface of sintered silver and SiC chip, and no metallization layer is considered. The energy release rate of interfacial crack between sintered silver and SiC chip is considered. The variations of energy release rate with crack depth with different sintered silver thicknesses are given in Fig. 2. Four different thickness of sintered silver are considered, i.e. 40 μm, 60 μm, 80 μm and 100 μm.

From Fig. 2, it is found that the effect of sintered silver thickness on the energy release rate is remarkable. In general, the thicker of the sintered silver layer, the higher value of the energy release rate will reach. With the increase of the crack length, the energy release rate of interfacial crack between sintered silver and SiC chip will increase firstly. If the crack length still grows, the energy release rate of the interfacial crack between sintered silver and SiC chip will become stable. The steady values of energy release rate of interfacial crack are 0.0836 N/mm, 0.079 N/mm, 0.0745 N/mm and 0.0703 N/mm, respectively.

For a specific sintered silver and SiC chip layer, the critical energy release rate is assured. The results show that the interfacial crack at $h_3 =$ 40 μm will extend more easily as the energy release rate is much easier to exceed the critical energy release rate. It indicates that the cracking risk of thinner sintered silver layer is higher.

The variations of phase angle for interfacial crack between sintered silver layer and SiC are shown in Fig. 3. It is seen that variations of phase angle generally increases from negative phase angle and then decreases with the increase of the crack depth and the finally reaches to a steady value. It also shows that the thinner of the sintered silver layer, the higher of the phase angle it will approach. In general, the interface cracking presents a mixed mode case and much close to the shearing mode.

To consider the metallization layer thickness effect on the crack tip energy release rate, the computations of energy release rate with different layer thicknesses are presented in Fig. 4. Five different thicknesses of metallization layers are considered in this paper. Compared with the calculated solutions, it can be found that the lowest values of energy release rate of metallization layer is the case with thickest Ni layer with 5 μm Ag layer. The highest energy release rate approaches when the thickness of metallization layer become 0.7 μm and 1.0 μm. It represents that the increase of metallization thickness will lead to the reduction of energy release rate to some extent. Similarly, the energy release rate of interfacial crack will become unchanged when the length of the interfacial crack exceeds 0.6.

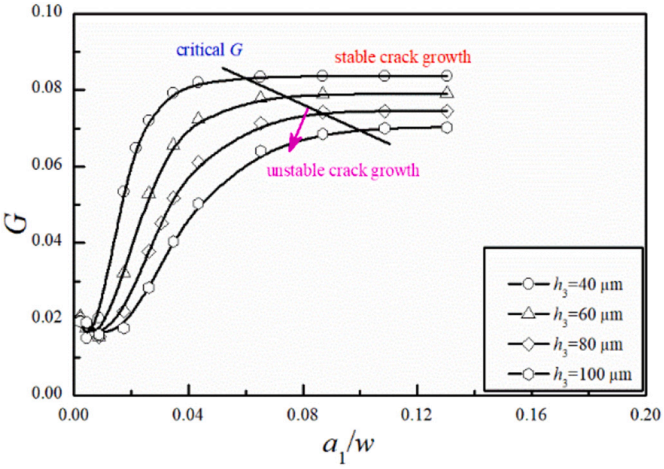

Fig. 2. Variations of energy release rate of interfacial crack along sintered Ag/SiC interface with different sintered silver layer thicknesses.

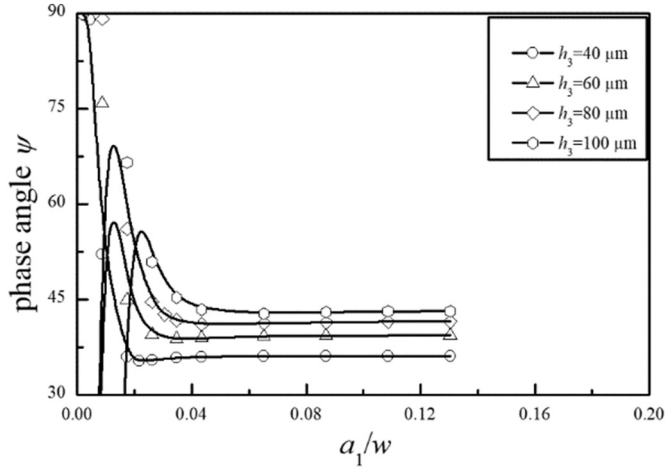

Fig. 3. Variations of phase angle for interfacial crack along Ag/SiC interface with different sintered silver layer thicknesses.

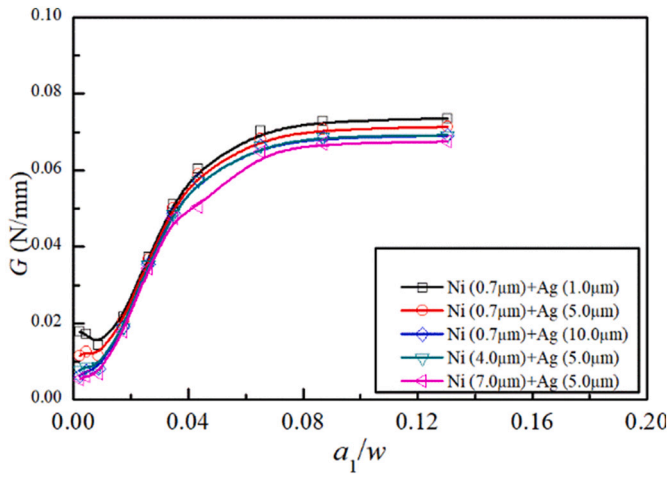

Fig. 4. Variations of energy release rate of interfacial crack with different metallization thicknesses.

3.2. Interfacial cracking of sintered Ag/Cu interface

Except for the interfacial cracking of sintered silver and SiC chip layer, cracking could also occur along the interface of Ag/Cu. The variations of energy release rate with different metallization conditions are shown in Fig. 5. Herein, a_1 is still the length of the interfacial crack. w is still the width of the die attach layer.

According to Fig. 5(a), the energy release rate of the interfacial crack generally increases with the increase of the die attach layer thickness. For thinner sintered silver layer, the energy release rate will be higher. If the interfacial crack between sintered silver and bare copper is shorter, the variations of energy release rate will change differently. For example, the energy release rate of interfacial crack at $h_3 = 100$ μm increases firstly and decreases slightly, then the energy release rate will increase to reach a steady value. It indicates that the thicker of the die attach layer and the energy release rate of interfacial crack between sintered silver and bare copper will be higher at deep crack length.

From Fig. 5(b), the influences of the Ni layer thickness and Au layer thickness on the energy release rate of interfacial crack are not that remarkable. It represents that the adding of Ni layer and Au layer will almost not affect the energy release rate of the interfacial crack. Although the numerical simulation shows the rule of Ni layer and Au layer is not the main factor which affect the energy release rate of the interfacial crack, however, the adding of Ni layer and Au layer may still play an important role on the strengthening of adhesive force between sintered silver and bare copper.

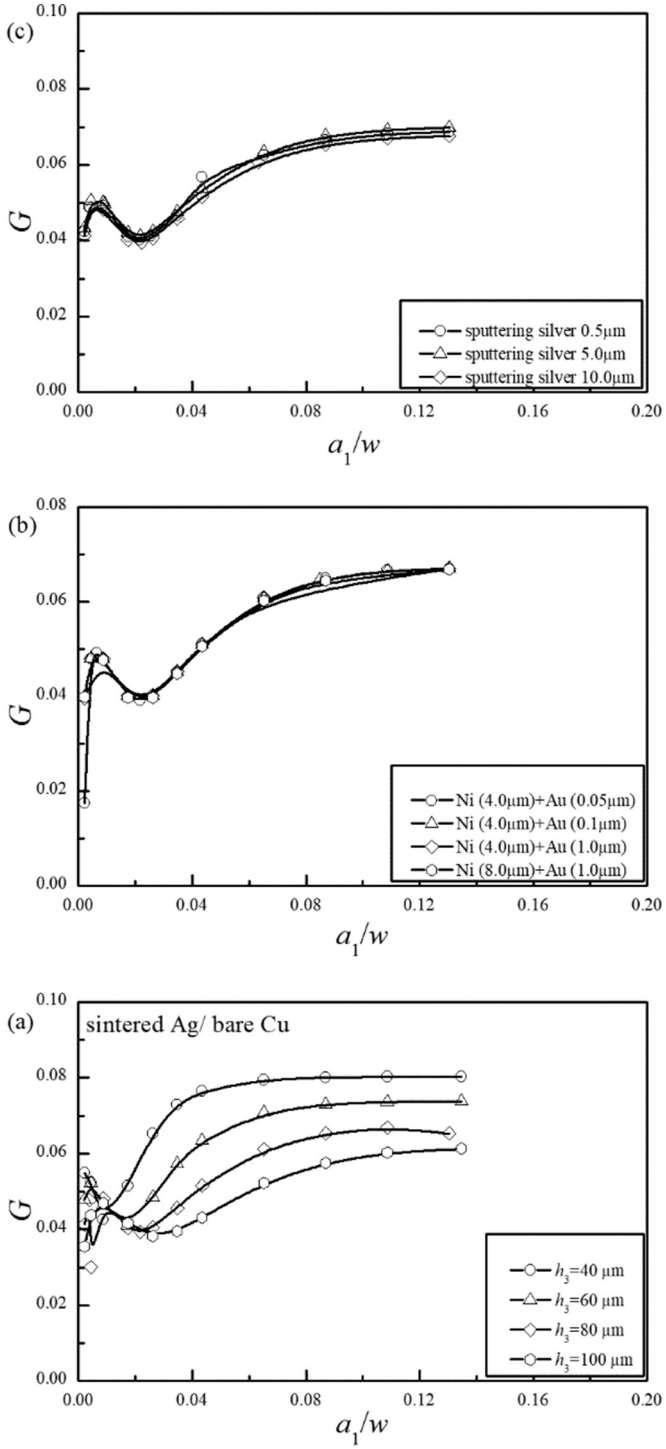

Fig. 5. Variations of energy release rate for interfacial crack along sintered silver/Cu interface (a) various sintered silver thicknesses; (b) various Ni and Au metallization layer and (c) sputtering silver layer.

If the metallization layer is changed to sputtering silver, similar tendencies of the variations of energy release rate are between Ni and Au layer as well as sputtering silver. With the increase of the thickness of the sputtering silver, the discrepancy of the energy release rate is not significant.

3.3. Vertical cracking

Another common cracking mode is the vertical crack emanating from the SiC chip side or copper baseplate side. Herein, the vertical cracking emanating from the SiC chip side is discussed firstly. The variations of the energy release rate of the vertical crack emanating from the SiC chip side are presented in Fig. 6. Three different sintered silver layer thicknesses are adopted to perform the numerical simulation, i.e. 40 μm, 60 μm and 80 μm, respectively. For those cases, the crack length of the vertical crack and the thickness of the sintered silver layer are denoted as a_2 and h_3, respectively. Three different locations for the crack are considered, i.e. left, middle and right side of the sintered silver layer. The distance of the left side vertical crack, middle side vertical crack and right side vertical crack to the left edge are 0.2 mm, 1.15 mm and 2.1 mm, respectively.

From Fig. 6(a), i.e. cracking emanating from the copper baseplate side, it can be seen that the highest energy release rate appears at h_3 = 40μm in the left side location. It indicates that the energy release rate of the vertical crack appearing in the left side, which is much higher than those of the other locations even with the same sintered silver layer thickness. For the same crack location, the energy release rate of vertical crack decreases with the increase of the sintered silver layer thickness. The lowest energy release rate among those vertical cracking conditions are the middle cracking case of the simulated sintered silver layer at h_3 = 40μm. It implies that the most dangerous cracking case appears at the left side of the sintered silver which should be avoided in the manufacturing or reliability evaluation. For cases with h_3 = 60μm and h_3 = 80μm, similar tendencies can be found to the cases with h_3 = 40μm, i.e. the left side vertical cracking condition possesses the highest energy release rate. Otherwise the vertical cracking in the middle location possesses the lowest energy release rate.

From Fig. 6(b), i.e. cracking emanating from the SiC chip side, it can be seen that the highest energy release rate also appears at h_3 = 40μm in the left side location. Again, the energy release rate of the vertical crack increases with the increase of crack length. The lowest energy release rate appears at the vertical cracking in the middle of the sintered silver layer.

Comparing with the values of the energy release rate, the maximum energy release rate between those vertical cracking is almost the same between those cases emanating from SiC chip side and emanating from the copper base plate side. The lowest energy release rate is obtained under the middle crack location with h_3 = 40μm.

3.4. Metallization geometry on the vertical cracking

Another important factor affecting the cracking behavior of the vertical crack is the influence of metallization layer thickness. Fig. 7 is presented to show the effect of metallization layer on the energy release rate of the vertical cracking. From Fig. 7(a), it can be seen that the thicker of the sputtering silver, the energy release rate will be higher. Comparing with the values of energy release rate of vertical crack with sputtering silver metallization layer, the values of energy release rate of vertical crack with Ni and Au layers are slight lower although the difference is not that remarkable. With the increase of the crack length, the energy release rate improves significantly.

From Fig. 7(b), i.e. crack emanating from the copper baseplate side, it can be found that the highest energy release rate of vertical cracking is

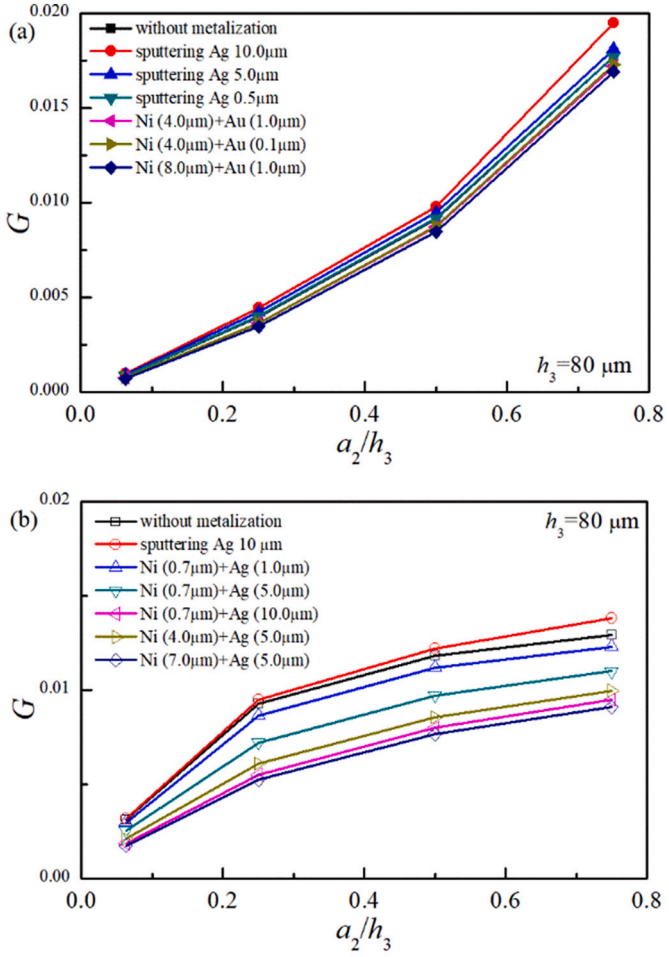

Fig. 7. Variations of energy release rate for vertical cracking with different metallization thickness (a) crack from the sintered silver and (b) crack from the SiC chip side.

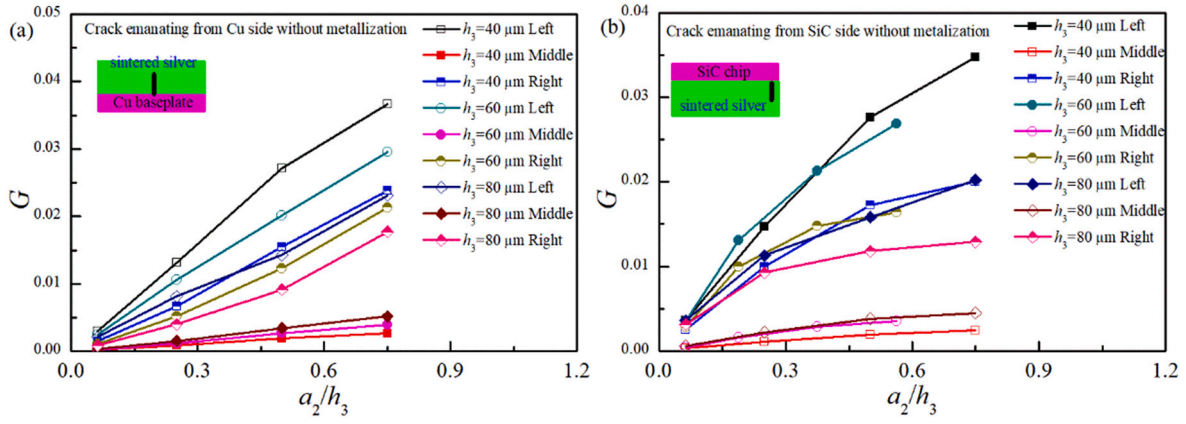

Fig. 6. Variations of energy release rate for vertical crack emanating from the SiC chip side: (a) with metallization; (b) without metallization;

still under the condition of sputtering silver with thickness of 10 μm. Generally, the values of energy release rate with Ni and Ag metallization layers are lower than those with sputtering silver layer. The increase of Ni layer enables to reduce the level of energy release rate. At the same time, the thicker of the Ni layer and the energy release rate will be lower. With the increase of crack length, the energy release rate become approaching to a stable value.

Comparing with those vertical crack emanating from the SiC chip side, the energy release rate of the vertical crack emanating from the copper baseplate side is slight higher if the crack length ratio is less than 0.4.

4. Discussions

4.1. Effect of porosity on the interface cracking

It has been given in Section 2 that the Young's modulus and Poisson's ratio are highly dependent on the porosity of the sintered silver. Hence, it is very necessary to investigate the porosity effect on the interface cracking as sintered silver are general porosity-dependent. It should be pointed out that the effect of porosity on mechanical properties contains many aspects, e.g. Young's modulus, Poisson's ratio and yielding strength. As the discussion in this paper are limited in linearly elastic condition, the main factors depending on porosity, i.e. Young's modulus and Poisson's ratio, are considered here. The variations of energy release rate with crack ratio are presented in Fig. 8 from which it is seen that the levels of energy release rate of sintered silver decreases with the increase of porosity. Note that the Poisson's ratio and Young's modulus of sintered silver at high porosity is smaller than those with low porosity. It implies that higher stiffer sintered silver with will lead to higher energy release rate. However, according to the experimental investigations given by Wang et al. [17], the fracture toughness of sintered silver is also a function of porosity and they found that the fracture toughness of sintered silver decreases with the increase of porosity. Hence, it implies that the cracking risk of sintered silver may need an evaluation between the reduction of porosity and reduction of fracture toughness.

4.2. Effect of porosity on vertical cracking

Except for the interface crack, the vertical cracking behaviors can be also caused by the variations of porosity of sintered silver. The variations of the energy release rate of vertical cracking are presented in Fig. 9. Herein, the vertical cracking of a left crack is adopted as the case to state the effect of porosity on vertical cracking of sintered silver. It is seen that the energy release rate of vertical crack generally increases with the augment of crack length. Similar to that of the interface crack, the vertical crack with higher porosity holds the relative higher energy release rate. It is noted that the energy release is also influenced by the thickness of the sintered silver. Thicker sintered silver will lead to lower energy release rate for vertical cracking.

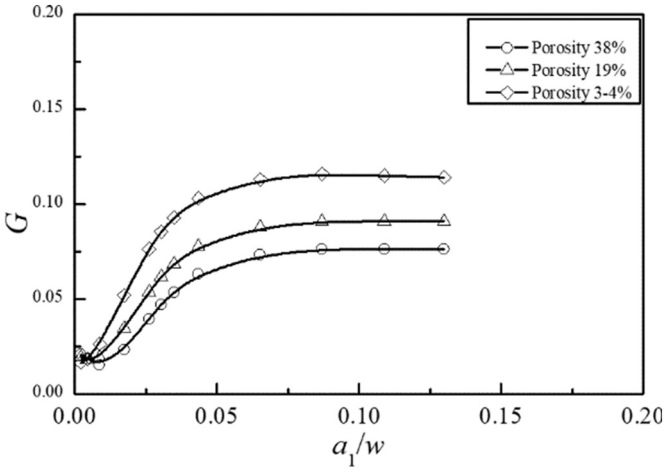

Fig. 8. Variations of energy release rate for interfacial cracking for sintered silver with different porosities.

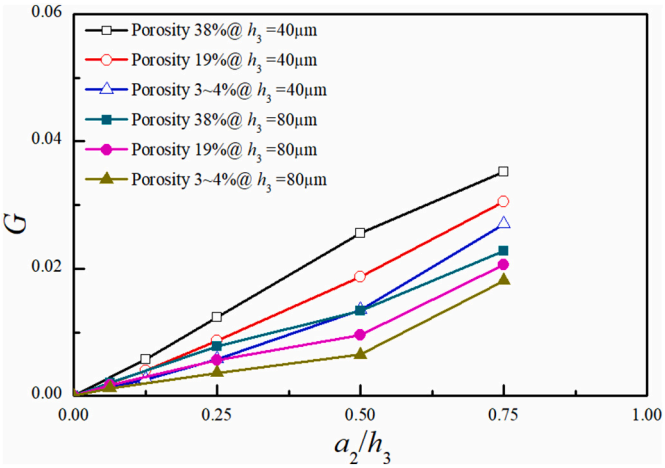

Fig. 9. Variations of energy release rate for vertical cracking with different porosities under different thicknesses.

4.3. Some hints obtained from the cracking simulation

Based on the numerical solutions, it is found that the most remarkable factor, which affects the energy release rate of interfacial crack, is the sintered silver thickness. In general, the thicker of the sintered silver layer, the higher of the energy release rate it will be, which implies that the formation of the interfacial crack is more easily in the thicker sintered silver layer.

Regarding to the metallization layer, the numerical solution shows that the adding of sputtering silver or Ni and Au layers does not change the energy release rate of the interfacial crack for interfacial crack between sintered silver and copper. Instead, the effect of metallization layer on the interfacial crack of sintered silver and SiC chip is relative more significant. It may indicate that the adding of metallization will not change the energy release rate of the interfaces in SiC/sintered silver/copper baseplate system remarkably, which means that the physical adhesive force is more important to be improved than energy release rate of interfacial crack by adding metallization layer. Many experiments have demonstrated that the interfacial crack forms more easily in sintered silver layer rather than those cases with interfaces of metallization layers. It should be noted that not all metallization layer materials are preferred as the adhesive force of those interfacial layers depends on the lattice structure of the materials among different layers.

For vertical cracking, the energy release rate depends on the crack location, crack origin as well as metallization layer. The thicker of the sputtering silver, the energy release rate will be higher. The adding of Ni metallization layer can help to reduce the level of energy release rate to some extent. For the vertical cracking, the vertical cracks emanating at the left side of the sintered silver layer may be more critical which should be considered carefully. However, the porosity effect is also important on the contribution of cracking behaviors as the variation tendencies for sintered silver with different porosities are different for interfacial cracking and vertical cracking according to our numerical investigations.

5. Conclusions

Through numerical simulation with rigorous fracture mechanics based modelling, the effect of metallization on different cracked

conditions of sintered silver layer under thermal loading are studied. The conclusions are obtained as following.

a) The most important factor which influences the energy release rate for interface cracks along the interfacial system of interconnection layers for SiC power devices is the thickness of sintered silver. The adding of metallization layer does not improve the energy release rate of the interface crack significantly although the energy release rate can be slightly influenced by the thickness of metallization layer. It indicates that the most important role of the metallization layer is the contribution to improve the adhesive force rather than improvement of the energy release rate.
b) For interface cracks, the values of energy release rate are very close regardless of the interface crack along sintered silver and copper interface or the interface crack along the SiC chip and sintered silver layer. Generally, the energy release rate of the interface crack heightens with increase of sintered silver layer thickness. The influence of metallization layer on the energy release rate of interface crack is in a limited level.
c) For the vertical crack, the level of energy release rate is strongly dependent on the crack location. The vertical crack near the chip edge shows the highest energy release rate. The vertical crack in the middle region of the simulated model presents the lowest energy release rate. The adding of the Ni layer enables to lower down the level of energy release rate of vertical crack.
d) The porosity effects of sintered silver on the interface cracking and vertical cracking are also studied. It is found that the higher porosity will lead to higher energy release rate for vertical cracking. However, the higher porosity will lead to lower energy release rate for interface cracking. It is also confirmed that the energy release rate of vertical crack are both influenced by thickness of sintered silver as thicker sintered silver could lead to lower energy release rate if the porosity effect is taken into account.

CRediT authorship contribution statement

Fei Qin: Methodology, Writing-Original Draft, Investigation, Project administration.

Shuai Zhao: Methodology, Software, Investigation, Writing- Review & Editing.

Lingyun Liu: Data curation, Investigation, Methodology, Software.

Yanwei Dai: Conceptualization, Visualization, Writing-Original Draft, Funding acquisition, Supervision.

Tong An: Writing- Review & Editing.

Pei Chen: Writing- Review & Editing.

Yanpeng Gong: Writing- Review & Editing.

Declaration of competing interest

The authors declare that they have no conflict of interest.

Acknowledgement

The authors acknowledge the supports from Beijing Natural Science Foundation (No. 2204074), National Natural Science Foundation of China (No. 11902009), and Scientific Research Common Program of Beijing Municipal Commission of Education (No. KM202010005034).

References

[1] F. Arabi, T. Youssef, M. Coudert, G. Coquery, N. Alayli, D. Martineau, O. Belnoue, Thermo-mechanical assessment of silver sintering for attaching power components in embedded PCB, Microelectron. Reliab. 114 (2020), 113900.
[2] K.S. Siow, Are sintered silver joints ready for use as interconnect material in microelectronic packaging? J. Electron. Mater. 43 (4) (2014) 947–961.
[3] H. Zhang, Z. Zhao, G. Zou, W. Wang, L. Liu, G. Zhang, Y. Zhou, Failure analysis and reliability evaluation of silver-sintered die attachment for high-temperature applications, Microelectron. Reliab. 94 (2019) 46–55.
[4] S. Noh, H. Zhang, J. Yeom, C. Chen, C. Li, K. Suganuma, Large-area die-attachment by silver stress migration bonding for power device applications, Microelectron. Reliab. 88 (2018) 701–706.
[5] T. Dale, Y. Singh, I. Bernander, G. Subbarayan, C. Handwerker, P. Su, B. Glasauer, Fatigue life of Sn3. 0Ag0. 5Cu solder alloy under combined cyclic shear and constant tensile/compressive loads, J. Electron. Packag. 142 (4) (2020), https://doi.org/10.1115/1.4048109.
[6] J.H. Lau, State of the art of lead-free solder joint reliability, J. Electron. Packag. 143 (2) (2021), 020803.
[7] T. Herboth, M. Guenther, A. Fix, J. Wilde, Failure mechanisms of sintered silver interconnections for power electronic applications, in: 2013 IEEE 63rd Electronic Components and Technology Conference, 2013, pp. 1621–1627.
[8] S. Kraft, A. Schletz, M. Maerz, Reliability of silver sintering on DBC and DBA substrates for power electronic applications, in: 2012 7th International Conference on Integrated Power Electronics Systems (CIPS), 2012, pp. 1–6.
[9] Y. Tan, X. Li, G. Chen, Y. Mei, X. Chen, Three-dimensional visualization of the crack-growth behavior of nano-silver joints during shear creep, J. Electron. Mater. 44 (2) (2015) 761–769.
[10] J. Dai, J. Li, P. Agyakwa, M. Corfield, C.M. Johnson, Comparative thermal and structural characterization of sintered nano-silver and high-lead solder die attachments during power cycling, IEEE Trans. Device Mater. Reliab. 18 (2) (2018) 256–265.
[11] M. Keikhaie, M.R. Movahhedy, J. Akbari, H. Alemohammad, Numerical study of material properties, residual stress and crack development in sintered silver nano-layers on silicon substrate, Sci. Iran. Trans. B Mech. Eng. 23 (3) (2016) 1037.
[12] P. Agyakwa, J. Dai, J. Li, B. Mouawad, L. Yang, M. Corfield, C.M. Johnson, Three-dimensional damage morphologies of thermomechanically deformed sintered nanosilver die attachments for power electronics modules, J. Microsc. 277 (3) (2020) 140–153.
[13] Y. Tan, X. Li, Y. Mei, G. Chen, X. Chen, Temperature-dependent dwell-fatigue behavior of nanosilver sintered lap shear joint, ASME. J. Electron. Packag. 138 (2) (2016), 021001, https://doi.org/10.1115/1.4032880.
[14] R. Shioda, Y. Kariya, N. Mizumura, K. Sasaki, Low-cycle fatigue life and fatigue crack propagation of sintered ag nanoparticles, J. Electron. Mater. 46 (2) (2017) 1155–1162.
[15] R. Kimura, Y. Kariya, N. Mizumura, K. Sasaki, Temperature dependence of fatigue crack propagation rate of pressureless sintered Ag nanoparticles, in: IEEE. 5th International Workshop on Low Temperature Bonding for 3D Integration (LTB-3D), 2017, p. 86.
[16] Koji Osaki, Yoshiharu Kariya, Noritsuka Mizumura, Koji Sasaki, High temperature fatigue crack propagation characteristics of pressureless sintered silver nanoparticles, in: IEEE 6th International Workshop on Low Temperature Bonding for 3D Integration (LTB-3D), 2019.
[17] S. Wang, C. Kirchlechner, L. Keer, G. Dehm, Y. Yao, Interfacial fracture toughness of sintered hybrid silver interconnects, J. Mater. Sci. 55 (7) (2020) 2891–2904.
[18] C. Chen, S. Nagao, K. Suganuma, J. Jiu, T. Sugahara, H. Zhang, K. Tsuruta, Macroscale and microscale fracture toughness of microporous sintered ag for applications in power electronic devices, Acta Mater. 129 (2017) 41–51.
[19] D. Kim, S. Lee, C. Chen, S.J. Lee, S. Nagao, K. Suganuma, Fracture mechanism of microporous Ag-sintered joint in a GaN power device with Ti/Ag and Ni/Ti/Ag metallization layer at different thermo-mechanical stresses, J. Mater. Sci. (2021) 1–19.
[20] F. Qin, Y. Hu, Y.An Dai, Chen P. T Gong Y and Yu H., Crack effect on the equivalent thermal conductivity of porously sintered silver, J. Electron. Mater. 49 (2020) 5994–6008.
[21] Tiam Foo Chen, Kim Shyong Siow, Comparing the mechanical and thermal-electrical properties of sintered copper (Cu) and sintered silver (Ag) joints, J. Alloys Compd. 866 (2021), 158783.
[22] Kim Shyong Siow, Mechanical properties of nano-silver joints as die attach materials, J. Alloys Compd. 514 (2012) 6–19.
[23] Andrew A. Wereszczak, Daniel J. Vuono, Hsin Wang, Mattison K. Ferber, Zhenxian Liang, Properties of Bulk Sintered Silver As a Function of Porosity, 2012. ORNL/TM-2012/130.
[24] D.J. DeVoto, P.P. Paret, A.A. Wereszczak, in: Stress Intensity of Delamination in a Sintered-silver Interconnection Additional Conferences (Device Packaging, HiTEC, HiTEN, and CICMT) 2014, 2014, pp. 190–197.
[25] Paul Paret, Power electronics materials and bonded interfaces – reliability and lifetime, National Renewable Energy Laboratory, 2020. https://www.nrel.gov/docs/fy20osti/76672.pdf.
[26] Dongjin Kim, Chuantong Chen, Seung-Joon Lee, Shijo Nagao, Katsuaki Suganuma, Strengthening of DBA substrate with Ni/Ti/Ag metallization for thermal fatigue-resistant Ag sinter joining in GaN power modules, J. Mater. Sci. Mater. Electron. 31 (4) (2020) 3715–3726.
[27] K. Sugiura, T. Iwashige, K. Tsuruta, C. Chen, S. Nagao, T. Funaki, K. Suganuma, Reliability evaluation of SiC power module with sintered ag die attach and stress-relaxation structure, IEEE Trans. Compon. Packag. Manuf. Technol. 9 (4) (2019) 609–615.
[28] C. Weber, H. Walter, M. Van Dijk, M. Hutter, O. Wittler, K.D. Lang, Combination of experimental and simulation methods for analysis of sintered Ag joints for high

temperature applications, in: 2016 IEEE 66th Electronic Components and Technology Conference (ECTC), 2016, pp. 1335–1341.

[29] H.N. Pishkenari, F.S. Yousefi, A. Taghibakhshi, Determination of surface properties and elastic constants of FCC metals: a comparison among different EAM potentials in thin film and bulk scale, Mater. Res. Express 6 (1) (2018), 015020.

[30] Y. Dai, M. Zhang, F. Qin, P. Chen, T. An, Effect of silicon anisotropy on interfacial fracture for three dimensional through-silicon-via (TSV) under thermal loading, Eng. Fract. Mech. 209 (2019) 274–300.